e-ISSN: 2687-6698 **Research Article**

Turkish Journal of Analytical Chemistry
www.turkjac.org
2019
TurkJAC

A "Turn-off" fluorescence sensor for Fe^{2+}, Fe^{3+}, and Cu^{2+} ions based on novel pyrene-functionalized chitosan

İpek Ömeroğlu*, Vildan Şanko

Gebze Technical University, Faculty of Science, Department of Chemistry, 41400, Kocaeli, Türkiye

Abstract

The detection of iron and copper ions is very important for environmental and biological processes. In this work, a novel pyrene-functionalized Schiff base chitosan (**Chit-Pyr**) was synthesized, and this hybrid material was used as a "turn-off" fluorescence sensor for the detection of Fe^{2+}, Fe^{3+}, and Cu^{2+} ions. FTIR, UV-Vis, TGA, and SEM were used to examine for structural, thermal, and morphological properties of **Chit-Pyr**. This sensor exhibited a selectivity towards Fe^{2+}, Fe^{3+}, and Cu^{2+} ions among several common metal cations in the DMF dispersion. The results showed that the proposed "turn-off" fluorescence sensing mechanism of **Chit-Pyr** was simple and sensitive for the determination of Fe^{2+}, Fe^{3+}, and Cu^{2+} ions.

Keywords: Fluorescence sensor, iron and copper, chitosan, pyrene

1. Introduction

Improving sensors for the detection and determination of transition metal ions is very important for environmental and biological processes [1]. Iron and copper ions, which are biological metals, play significant roles in these processes [2–4]. Iron exists in the form of ferrous (Fe^{2+}) and ferric (Fe^{3+}) ions and is indispensable in physiological processes such as oxygen binding, respiration, and enzymatic reactions [5–8]. Although it is of great importance in physiological processes, iron deficiency causes diabetes, anemia, liver, heart, and kidney damage, and iron accumulation causes serious diseases such as cancer, Parkinson's, and Alzheimer's [9–11]. Copper is the third most abundant transition metal in the human body, and excess copper in the human body causes diseases such as vomiting, increased blood pressure and respiratory rate, acute hemolytic anemia, and liver damage [12]. Therefore, it is very important to improve simple, sensitive, fast, cost-effective, and portable alternating for metal ion definition [13]. Many analytical techniques such as high-performance liquid chromatography (HPLC), anodic stripping voltammetry, inductively coupled plasma-mass spectrometry (ICP-MS), and atomic absorption spectrometry (AAS) have been improved for the definition of iron and copper [14–21]. In addition to traditional analytical methods, fluorescence probes have been widely used in recent years for the detection of any analyte [22]. Fluorescence probes are of great interest for applications such as optical imaging and analytical sensing due to their high sensitivity, simplicity, and fast response times [23]. Fluorescence detection, which has turned into an effective tool for real-time detection and monitoring of biological species and physiological processes, is non-invasive, well-operative, and extremely susceptible [24].

Biopolymers, which can be divided into natural and synthetic based on their origin, are long chain-like molecules containing repeating monomer units that are environmentally degradable [25,26]. Cellulose, chitosan, and chitin are polysaccharide derivative biopolymers in the natural biopolymer class [27]. Chitosan, the second most abundant biopolymer on Earth after cellulose, is a polycationic polysaccharide derived from chitin, consisting of *N*-acetyl-d-glucosamine units linked by β-(1,4)-glycosidic bonds [28,29]. It is soluble in aqueous solutions such as acetic acid and lactic acid, and its solubility depends on the degree of deacetylation (DD) and molecular weight [30]. It is used in many applications due to its non-toxic, low-cost, versatility,

Citation: İ. Ömeroğlu, V. Şanko, A "Turn-off" Fluorescence Sensor for Fe^{2+}, Fe^{3+}, and Cu^{2+} Ions Based on Novel Pyrene-Functionalized Chitosan, Turk J Anal Chem, 5(1), 2023, 50–60.

https://doi.org/10.51435/turkjac.1302873

***Author of correspondence:** iomeroglu@gtu.edu.tr
Tel: +90 (262) 605 31 11
Fax: +90 (262) 605 30 05

Received: May 26, 2023
Accepted: June 08, 2023

biodegradability, biocompatibility, digestibility, antibacterial, anti-tumor, hemostatic, and antioxidant properties [31–34]. Chitosan has shortcomings such as low mechanical properties, thermal stability, and high sensitivity to moisture. To overcome these shortages, chitosan is functionalized using physical, chemical, and biological modification methods [30]. Also, in fluorescence sensor applications, the fact that it does not have fluorescence properties requires modification with new groups.

Pyrene, one of the polyaromatic hydrocarbon family, is widely used as a fluorescence probe in many applications. It is well-known that pyrene and its derivatives show both monomeric and excimer fluorescence emission [35]. The pyrene displays the monomer emission wavelength in the range of ~380–410 nm and the excimer emission wavelength in the range of ~450–500 nm [36]. The formation of the excimer causes the emission wavelength of the pyrene compound to exhibit a bathochromic shift to a longer wavelength [37]. Excimer emission of pyrene due to interactions between pyrene units, one of which is excited, both in the solution and in the solid state under different conditions, may result from an intermolecular or intramolecular process [38]. Although pyrene-modified chitosan biopolymers have been reported in the literature, they differ from our study in terms of synthesis and application. Jatunov *et al.* synthesized a biopolymer expressing molecules with different physicochemical properties by adding equimolar amounts of aldehydes (4-*N*,*N*-diphenylaminobenzaldehyde, 4-*N*,*N*-dimethylamino-1-naphthaldehyde, and 1-pyrenecarboxaldehyde) to a methanolic suspension of chitosan [39]. Franconetti *et al.* developed aromatic and heteroaromatic aldehydes with malononitrile, a symmetric active methylene compound. Then, the catalytic activities of organocatalysts, chitosan hydrogel beads, and hydrogel disks formed by ureidyl-chitosan derivatives were evaluated as a function of pH, temperature, and catalyst concentration [40]. Sirajunnisa *et al.* synthesized the β-amino derivative of lawsone using chitosan and 1-pyrenecarboxaldehyde *via* the Mannich reaction. Also, they prepared quaternization of a Mannich base and following intercalation into bentonite clay produced the organic-inorganic hybrid systems [41]. However, as far as we know 1-pyrenecarboxaldehyde-modified chitosan prepared as a fluorescence sensor for the detection of metal ions is not yet available in the literature. In addition, chitosan and its derivatives are used in the fluorometric determination of various analytes. Although chitosan compound containing 1-pyrenecarboxaldehyde is not available in the literature, these biopolymers containing different fluorescent groups are used as a fluorescence sensor for the detection of metal ions [42–44].

In this work, novel pyrene-functionalized Schiff base chitosan was synthesized as a "turn-off" fluorescence determination of Fe^{2+}, Fe^{3+}, and Cu^{2+} ions. The characterization, morphological, and thermal properties of **Chit-Pyr** were investigated by FTIR, SEM, and TGA. The photophysical and fluorescence sensor properties were measured by UV-Vis and fluorescence spectroscopies. Also, the change of color was observed by adding Fe^{2+} and Fe^{3+} ions to the dispersion of **Chit-Pyr** in DMF. As a result, new photophysical, thermal, and morphological properties were gained to the biopolymer by functionalizing the chitosan with the pyrene compound.

2. Experimental

2.1. Materials and equipments

Chitosan, 1-pyrenecarboxaldehyde, glacial acetic acid, absolute ethanol (EtOH), dichloromethane (DCM), tetrahydrofuran (THF), acetonitrile (ACN), dimethyl sulfoxide (DMSO), dimethylformamide (DMF), $AgNO_3$, $BaCl_2$, $CaCl_2$, $CdCl_2$, CsCl, $CuCl_2$, $FeCl_2$, $FeCl_3$, $HgCl_2$, KCl, LiCl, $MgCl_2$, $MnCl_2$, NaCl, $PbCl_2$, and $ZnCl_2$ metal salts were obtained from commercial suppliers. Ultrapure water (18.2 MΩ) was used for chemical reaction and sensor measurements.

Fourier-transform infrared spectroscopy (FTIR) spectra were recorded on a Perkin Elmer Spectrum 100 spectrophotometer. Scanning Electron Microscopy (FEI, Nova Nano SEM 450) was used for the analysis of surface morphological properties. Thermogravimetric analysis (TGA) was performed by Thermal Analysis System (Mettler Toledo STARe) and the heating rate was adjusted to 10 °C/min when the N_2 flow rate was kept at 50 mL/min. Absorption spectra were recorded with a Shimadzu 2101 UV-Vis spectrophotometer. Fluorescence emission spectra were obtained by a Varian Eclipse spectrofluorometer.

2.2. Synthesis of pyrene-modified chitosan (Chit-Pyr)

0.50 g of low molecular weight chitosan was dissolved in 20 mL of ultrapure water and five drops of glacial acetic acid (AcOH). It was stirred at 50 °C for two hours to completely dissolve the chitosan. Then, an excess amount of 1-pyrenecarboxaldehyde dissolved in 10 mL of ethanol was added to the reaction mixture under an inert atmosphere and refluxed for 24 hours. After that time, the reaction solvent was removed and the solid product was washed several times with THF, DCM, and ethanol to remove unreacted 1-pyrenecarboxaldehyde. The light-yellow product was dried in a vacuum oven at 55 °C.

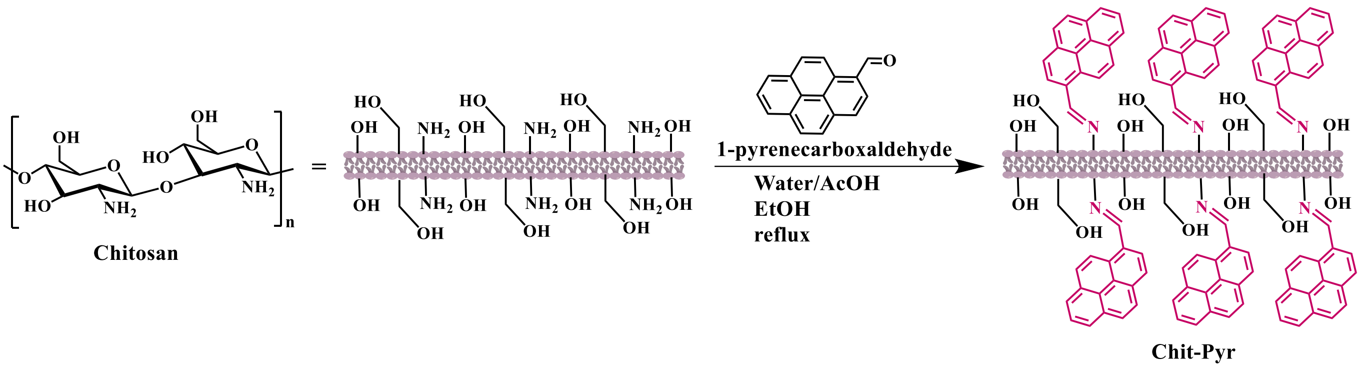

Scheme 1. The synthetic procedure of pyrene-modified chitosan (**Chit-Pyr**)

2.3. "Turn-off" fluorescence sensor measurements

Absorption and emission changes upon the addition of metal ions (Ag^+, Ba^{2+}, Ca^{2+}, Cd^{2+}, Cs^+, Cu^{2+}, Fe^{2+}, Fe^{3+}, Hg^{2+}, K^+, Li^+, Mg^{2+}, Mn^{2+}, Na^+, Pb^{2+}, Zn^{2+}) to the **Chit-Pyr** dispersion were determined using a UV-Vis and fluorescence spectrophotometer. Absorption and fluorescence emission spectra in "turn-off" fluorescence sensor measurements were performed **Chit-Pyr** in the DMF dispersion (0.4 mg/mL) at room temperature. The aqueous solutions of the metal chlorides (nitrate derivative for Ag^+ ion, 0.1 M) were used as the source of metal ions in these measurements. Spectra were routinely acquired at 25 °C in a 1 cm path-length quartz cuvette by adding 0.1 M different metal ions (Ag^+, Ba^{2+}, Ca^{2+}, Cd^{2+}, Cs^+, Cu^{2+}, Fe^{2+}, Fe^{3+}, Hg^{2+}, K^+, Li^+, Mg^{2+}, Mn^{2+}, Na^+, Pb^{2+}, Zn^{2+}) to 2 mL solution. The metal solutions used in the measurements were prepared as 0.1 M stock solutions in ultrapure water using metal salts ($AgNO_3$, $BaCl_2$, $CaCl_2$, $CdCl_2$, $CsCl$, $CuCl_2$, $FeCl_2$, $FeCl_3$, $HgCl_2$, KCl, $LiCl$, $MgCl_2$, $MnCl_2$, $NaCl$, $PbCl_2$, and $ZnCl_2$).

3. Results and discussion

3.1. Synthesis and characterization

Chitosan containing primary amine was substituted with pyrene, a fluorophore group with good photophysical properties, using a chemical modification method and utilized in the fluorescence detection platform. The pyrene-modified chitosan (**Chit-Pyr**) was synthesized *via* Schiff base reaction as a fluorescent sensor for "turn-off" fluorescence determination of Fe^{2+}, Fe^{3+}, and Cu^{2+} (Scheme 1).

The chemical, thermal, and morphological characterizations of the final product **Chit-Pyr** are given in Fig. 1.

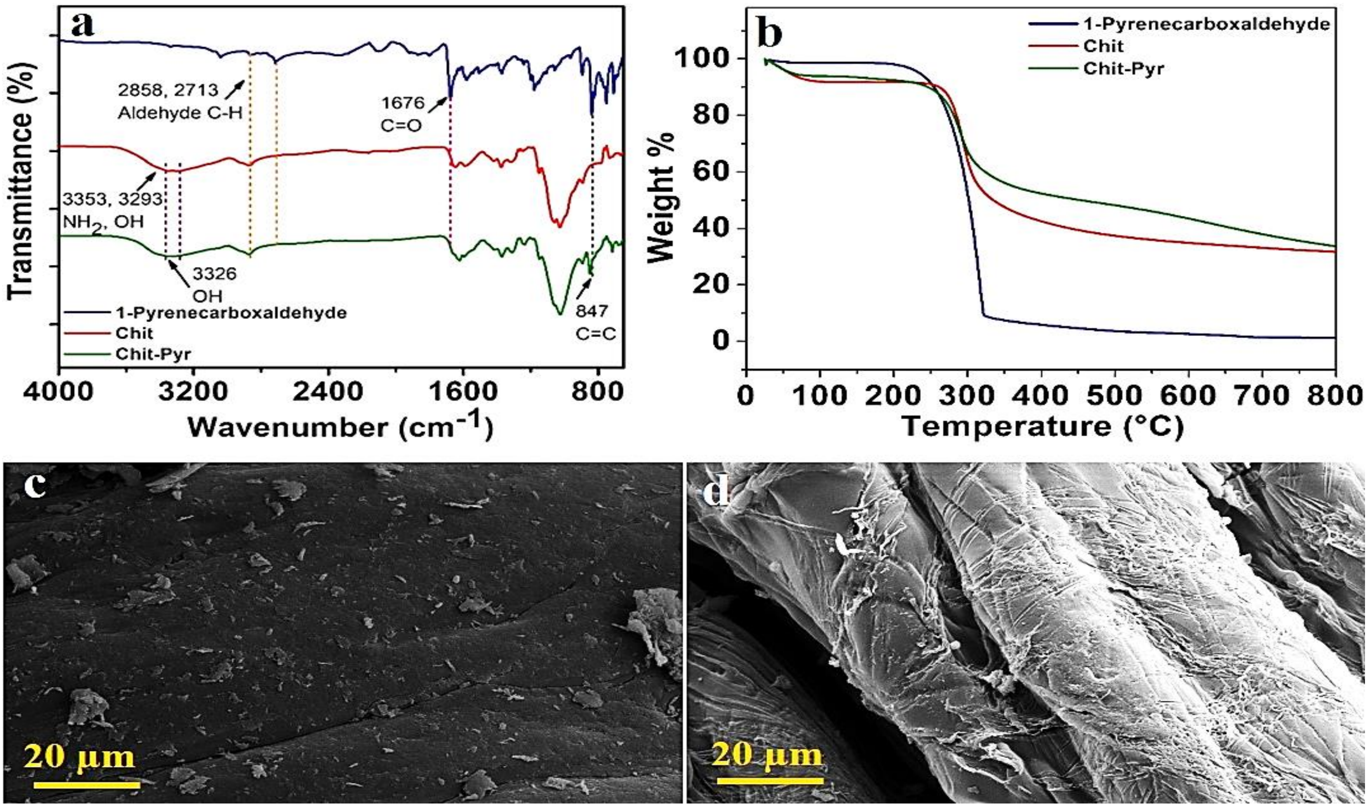

Figure 1. (a) FTIR spectra, (b) TGA diagrams of 1-pyrenecarboxaldehyde, Chit, **Chit-Pyr** and SEM images of (c) Chit and (d) **Chit-Pyr** surfaces with X1000 magnification

Also, the chemical and thermal characterizations of the starting compounds Chit and 1-pyrenecarboxaldehyde are shown in Fig. 1a–b. In the FTIR spectra (Fig. 1a), the peaks representing the 1-pyrenecarboxaldehyde structure, which is one of the starting materials, were detected by the literature. The presence of aldehyde C-H peaks at 2858–2713 cm^{-1} and C=O peak at 1676 cm^{-1} support the structure [45]. The characteristic peaks of the Chit structure, N-H and O-H peaks at 3353–3293 cm^{-1}, symmetrical and asymmetrical C-H stretching vibrations at 2880 cm^{-1}, C=O at 1657 cm^{-1} and C-O stretching vibrations at 1059 cm^{-1} confirm the structure [46]. In the FTIR spectrum of **Chit-Pyr**, which is the product obtained after modification, the peaks of chitosan are prominently present, while at the same time, the peak modification at 1623 cm^{-1} for the C-N bond vibration, which indicates the formation of Schiff base, confirms the modification [45].

Changes in the thermal properties of materials are also one of the important characterizations supporting whether the modification has taken place. Therefore, for this study, the thermal properties of the study groups were examined, and the thermal diagrams obtained are given in Fig. 1b. It has been determined that chitosan undergoes thermal decomposition at approximately 350 °C with a significant mass loss of 48%. 1-pyrenecarboxaldehyde lost about 90% of its mass at 323 °C. The temperature at which mass loss of **Chit-Pyr** was observed also showed similar characteristics with Chit. The fact that the thermal decomposition temperatures of the bonded organic group and Chit structures were very close caused the obtained product to undergo thermal decomposition at a similar temperature point. However, some variation in the percent mass loss was detected. A mass loss of 40% indicates that the thermal properties of the Chit structure increase after modification. In addition, the difference in the thermal course after the temperature range (350-800 °C) where rapid mass loss is observed supports the modification [47,48].

For morphological characterization, the images of chitosan particles before (Fig. 1c) and after (Fig. 1d) were modified with 1-pyrenecarboxaldehyde were examined. The surface of the chitosan particles appears to be smoother and relatively more homogeneous. In addition, it was determined that the surface of **Chit-Pyr** particles changed considerably to support the modification and had a rougher and non-homogeneous surface.

Normalized absorption spectra of 1-pyrenecarboxaldehyde, Chit, and **Chit-Pyr** in DMF were given in Fig. 2. As seen in Fig. 2, no apparent absorption peaks were monitored in the region of 270–570 nm in the UV-Vis absorption spectrum of Chit. After the chitosan was modified with pyrene (**Chit-Pyr**), the novel hybrid material showed a new absorption peak at 275–293 nm and 340–396 nm which were attributed to π-π* transitions of the pyrene moieties [49]. Thus, the absorption spectrum of the hybrid material (**Chit-Pyr**) confirmed that the pyrene has been modified to the chitosan surface.

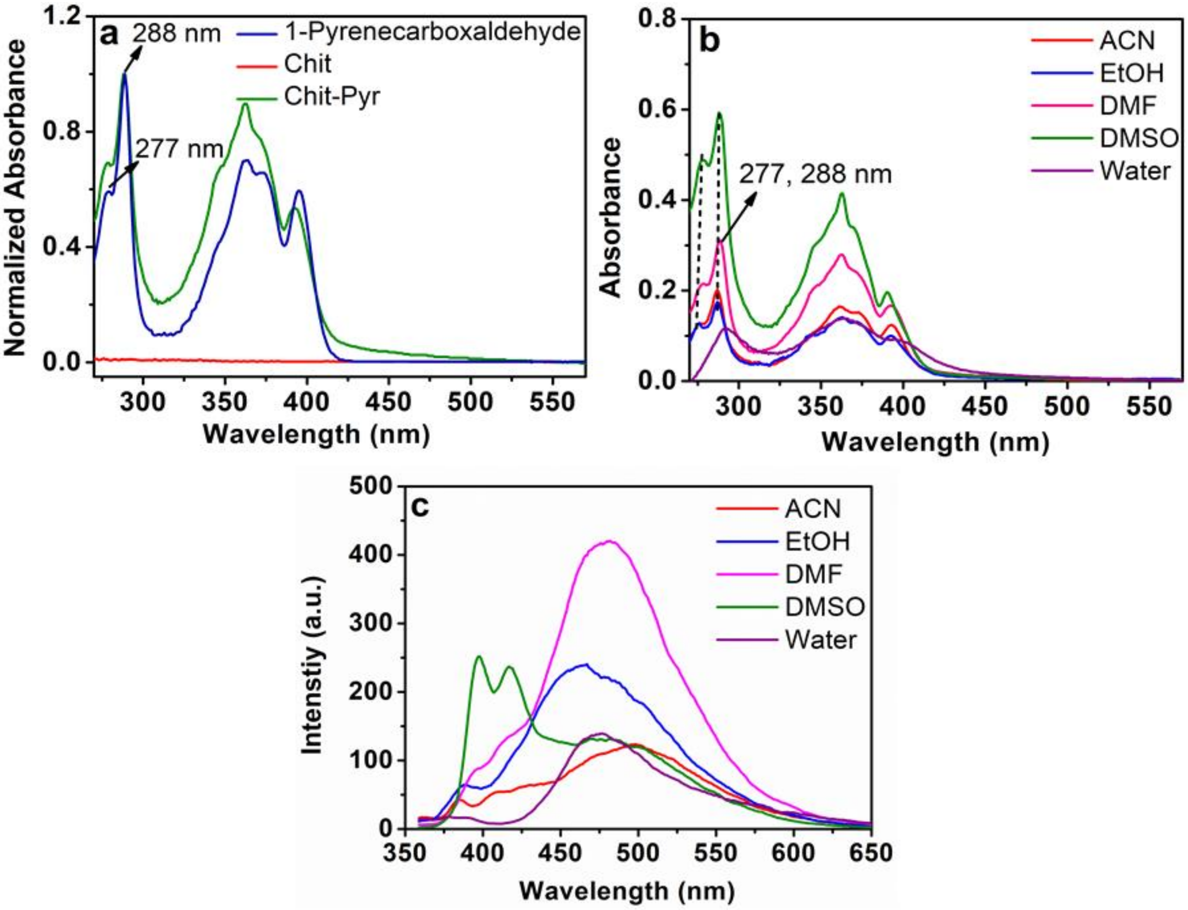

Figure 2. (a) Normalized UV-Vis absorption spectra of 1-pyrenecarboxaldehyde, Chit, and **Chit-Pyr** in DMF, (b) UV-Vis absorption spectra of 0.4 mg/mL **Chit-Pyr** in different solvents, and (c) fluorescence emission spectra of 0.4 mg/mL **Chit-Pyr** in different solvents (λ_{ex}=345 nm)

3.2. Photophysical studies

The absorption and fluorescence properties of pyrene-modified chitosan hybrid (**Chit-Pyr**) were investigated in different water-miscible solvents such as THF, ACN, EtOH, DMF, DMSO, and water at the same concentration (0.4 mg/mL, Fig. 2b–c). In addition, absorption and emission spectra of **Chit-Pyr** at different concentrations from 0.4 mg/mL to 0.1 mg/mL and in different solvents were measured to examine the effect of on the UV-Vis and emission absorption properties of **Chit-Pyr**. The absorbance values were decreased comparatively when the concentration of **Chit-Pyr** was decreased without a significant change in the absorption wavelength (Fig. 3).

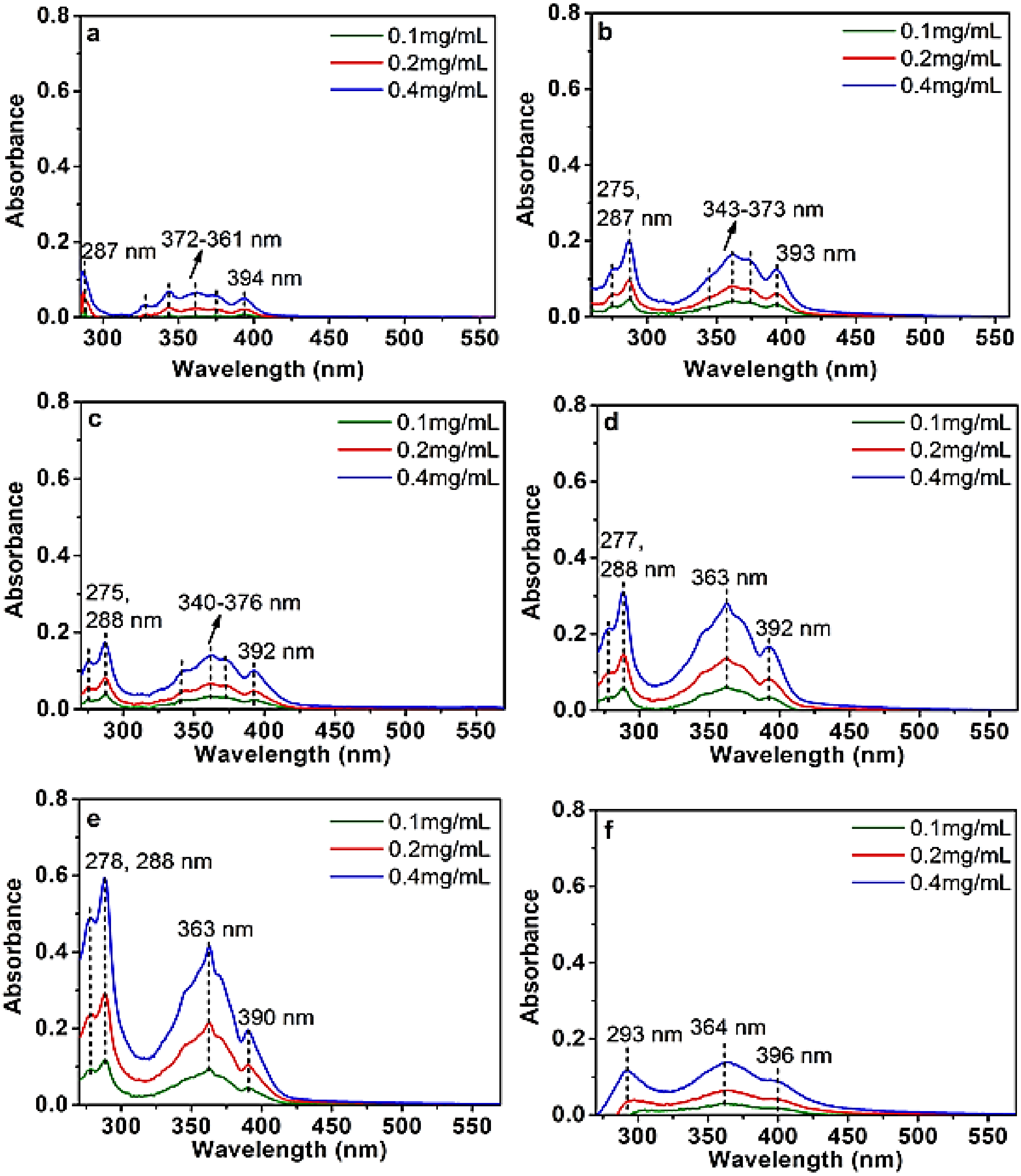

Figure 3. UV-Vis absorption spectra of Chit-Pyr in (a) THF, (b) ACN, (c) EtOH, (d) DMF, (e) DMSO, and (f) water at different concentrations

The emission characteristic of **Chit-Pyr** was investigated at different concentrations from 0.4 mg/mL to 0.1 mg/mL and in different solvents when excited at 345 nm (Fig. 4). It was determined that the excimer emission of **Chit-Pyr** obtained in ethanol and water, which are polar protic solvents, was blue-shifted compared to polar aprotic solvents [50]. In addition, emission bands of both monomer and excimer of the **Chit-Pyr** were obtained in solvents such as THF, ACN, EtOH, and DMSO. The emission intensity of the monomer emission (398 and 418 nm) was determined as DMSO higher than the excimer emission (481 nm) compared to other solvents. Also, the excimer *vs.* monomer emission intensity ratio (I_e/I_m) of **Chit-Pyr** in DMSO was calculated as ~0.6, and this ratio remained the same with increasing or decreasing concentration. Among all solvents studied, DMF was chosen as the solvent in "turn-off" fluorescence sensor studies, because **Chit-Pyr** showed a high emission peak in DMF which is miscible in water.

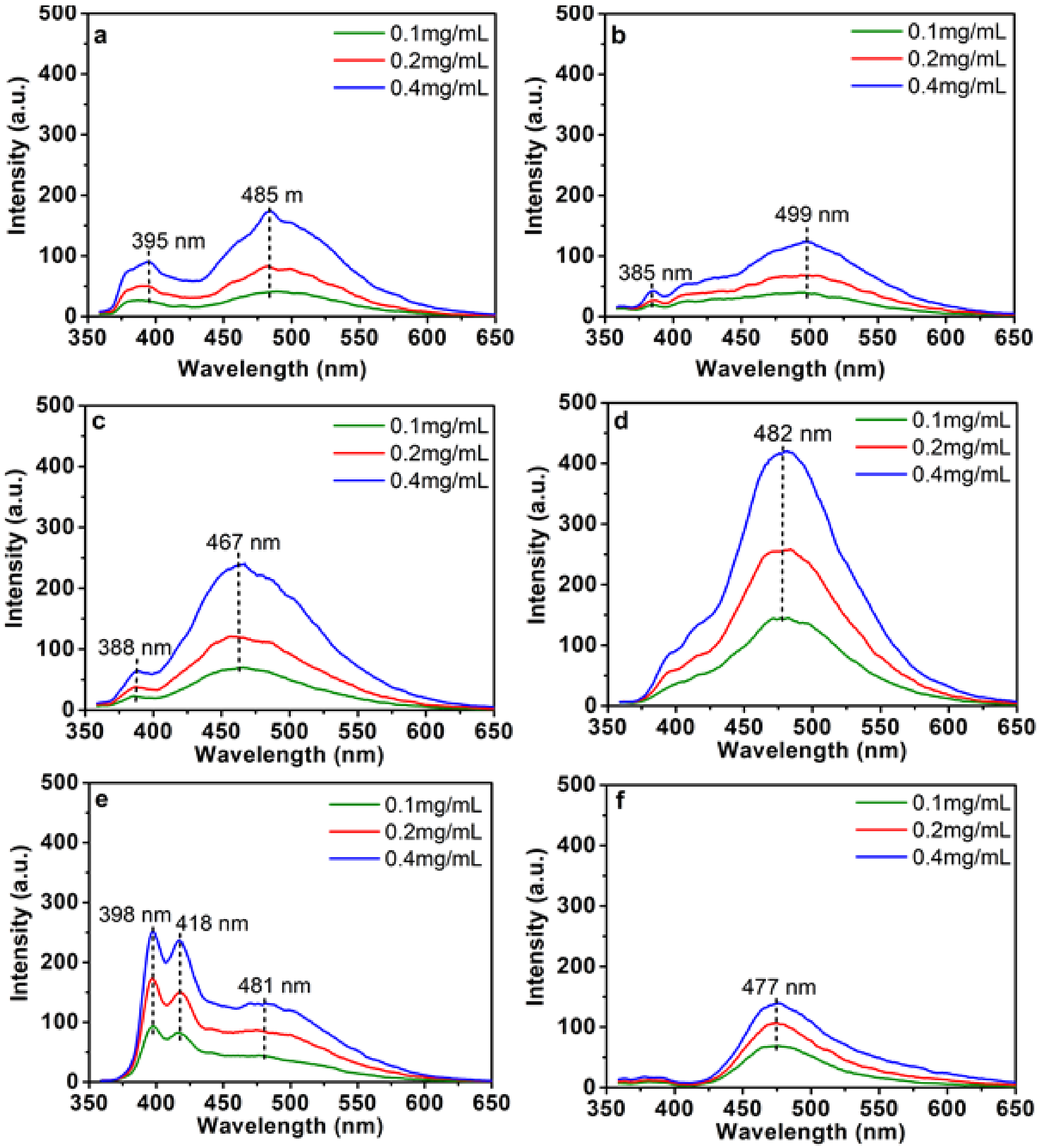

Figure 4. Fluorescence emission spectra of **Chit-Pyr** in (a) THF, (b) ACN, (c) EtOH, (d) DMF, (e) DMSO, and (f) water at different concentrations (λ_{ex}=345 nm)

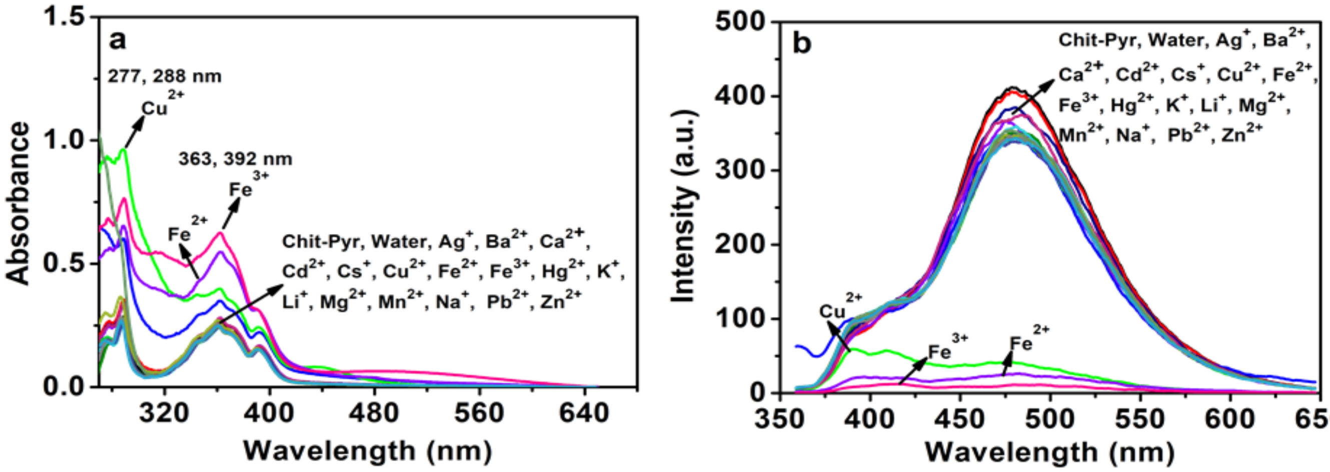

Figure 5. (a) UV-Vis absorption spectra and (b) fluorescence emission spectra of Chit-Pyr (0.4 mg/mL in DMF λ_{ex} = 345 nm) upon addition of 0.1 M of various metal ions (Ag^+, Ba^{2+}, Ca^{2+}, Cd^{2+}, Cs^+, Cu^{2+}, Fe^{2+}, Fe^{3+}, Hg^{2+}, K^+, Li^+, Mg^{2+}, Mn^{2+}, Na^+, Pb^{2+}, Zn^{2+})

3.3. "Turn-off" fluorescence sensor studies

The pyrene-modified chitosan (**Chit-Pyr**) was dispersed in DMF and "turn-off" fluorescence sensor studies were performed at a concentration of 0.4 mg/mL. **Chit-Pyr** was dispersed in DMF with an ultrasonic bath and 5 μL of 0.1 M of various metal ions (Ag^+, Ba^{2+}, Ca^{2+}, Cd^{2+}, Cs^+, Cu^{2+}, Fe^{2+}, Fe^{3+}, Hg^{2+}, K^+, Li^+, Mg^{2+}, Mn^{2+}, Na^+, Pb^{2+}, Zn^{2+}) were added to the dispersion of **Chit-Pyr**. Then, the absorption and emission responses of **Chit-Pyr** were evaluated after adding metal ions (Fig. 5). As seen in Fig. 5a, absorption properties of **Chit-Pyr** considerably changed after the addition of Fe^{2+}, Fe^{3+}, and Cu^{2+} ions to a dispersion of **Chit-Pyr**. The absorption peaks of **Chit-Pyr**, observed at 277 and 288 nm, were increased 2.9- and 2.3-fold for Fe^{2+}, 3.6- and 2.7-fold for Fe^{3+}, and 4.9- and 3.4-fold for Cu^{2+}, respectively. Also, the absorption peaks of **Chit-Pyr**, monitored at 363 and 392 nm, were increased 2.1- and 2.0-fold for Fe^{2+}, 2.4- and 2.0-fold for Fe^{3+}, and 1.5- and 1.5-fold for Cu^{2+}, respectively. No blue or red shifts were detected in the absorption bands with the addition of metal ions (Ag^+, Ba^{2+}, Ca^{2+}, Cd^{2+}, Cs^+, Cu^{2+}, Fe^{2+}, Fe^{3+}, Hg^{2+}, K^+, Li^+, Mg^{2+}, Mn^{2+}, Na^+, Pb^{2+}, Zn^{2+}).

The emission spectra of **Chit-Pyr** were obtained towards Fe^{2+}, Fe^{3+}, and Cu^{2+} ions at the same analytical conditions with absorption measurements. As shown in Fig. 5b, the emission bands of **Chit-Pyr** with moderate emission intensity at 482 nm were decreased 15.8-fold for Fe^{2+}, 37.4-fold for Fe^{3+}, and 10.3-fold for Cu^{2+}. No significant changes were determined in the emission band with the addition of other metals (Ag^+, Ba^{2+}, Ca^{2+}, Cd^{2+}, Cs^+, Hg^{2+}, K^+, Li^+, Mg^{2+}, Mn^{2+}, Na^+, Pb^{2+}, Zn^{2+}). The addition of other metals did not cause any significant changes in the emission band of **Chit-Pyr**.

As seen in Fig. 6a, the relative fluorescence response of **Chit-Pyr** confirmed the high selectivity of **Chit-Pyr** against Fe^{2+}, Fe^{3+}, and Cu^{2+} ions and showed that it was unaffected by competitive species. The addition of Fe^{2+}

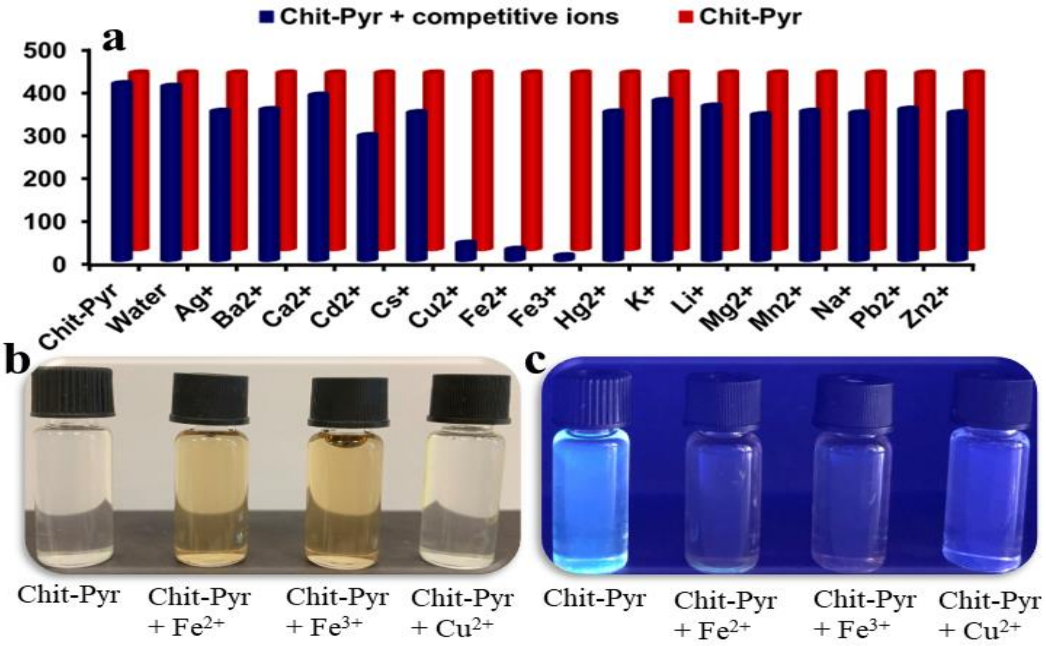

Chit-Pyr Chit-Pyr + Fe^{2+} Chit-Pyr + Fe^{3+} Chit-Pyr + Cu^{2+} Chit-Pyr Chit-Pyr + Fe^{2+} Chit-Pyr + Fe^{3+} Chit-Pyr + Cu^{2+}

Figure 6. (a) Fluorescence signal change of Chit-Pyr in DMF addition of various competitive ions, the color change of Chit-Pyr in DMF (0.4 mg/mL) (b) daylight, and (c) UV light

and Fe^{3+} ions to **Chit-Pyr** solution dispersed in DMF caused significant color changes to the naked eye (colorless to light brown, Fig. 6b) and under UV light (blue/green to colorless, Fig. 6c). While there was no visible color change after addition of Cu^{2+} was added, a color change from blue/green to colorless was observed under UV light (Fig. 6c). Thus, it was determined that the newly synthesized pyrene modified chitosan hybrid (**Chit-Pyr**) indicated "turn-off" fluorescence sensor properties against these metals. Also, the color change after the addition of Fe^{2+} and Fe^{3+} ions indicated that this hybrid material can be used as both a colorimetric and fluorometric sensor platform.

Fluorescence titration of **Chit-Pyr** with an increased amount of Fe^{2+}, Fe^{3+}, and Cu^{2+} ions was measured in DMF to define the linear "turn-off" response of the **Chit-Pyr** towards the selective metal ions (Fig. 7). The fluorescence signals of **Chit-Pyr** were gradually "turn-off" upon the addition of Fe^{2+}, Fe^{3+}, and Cu^{2+} ions, respectively.

The linear regression equation for selective metal ions was calculated as $y = -8.1857\,[Fe^{2+}] + 401.14$ ($R^2 = 0.9971$), $y = -9.4774\,[Fe^{3+}] + 424.94$ ($R^2 = 0.985$), and $y = -8.9291\,[Cu^{2+}] + 393.32$ ($R^2 = 0.9948$) (Fig. 8). The limit of detection (LOD) is calculated with 3σ/K where σ and K represent the standard deviation of the blank sample and slope of calibration curves, respectively. LODs were determined as 2.52 μM for Fe^{2+}, 1.74 μM for Fe^{3+}, and 1.96 μM for Cu^{2+}. Also, the limit of quantification (LOQ) for Fe^{2+}, Fe^{3+}, and Cu^{2+} were calculated as 7.56 μM, 5.21 μM and 5.89 μM with 9σ/K, respectively.

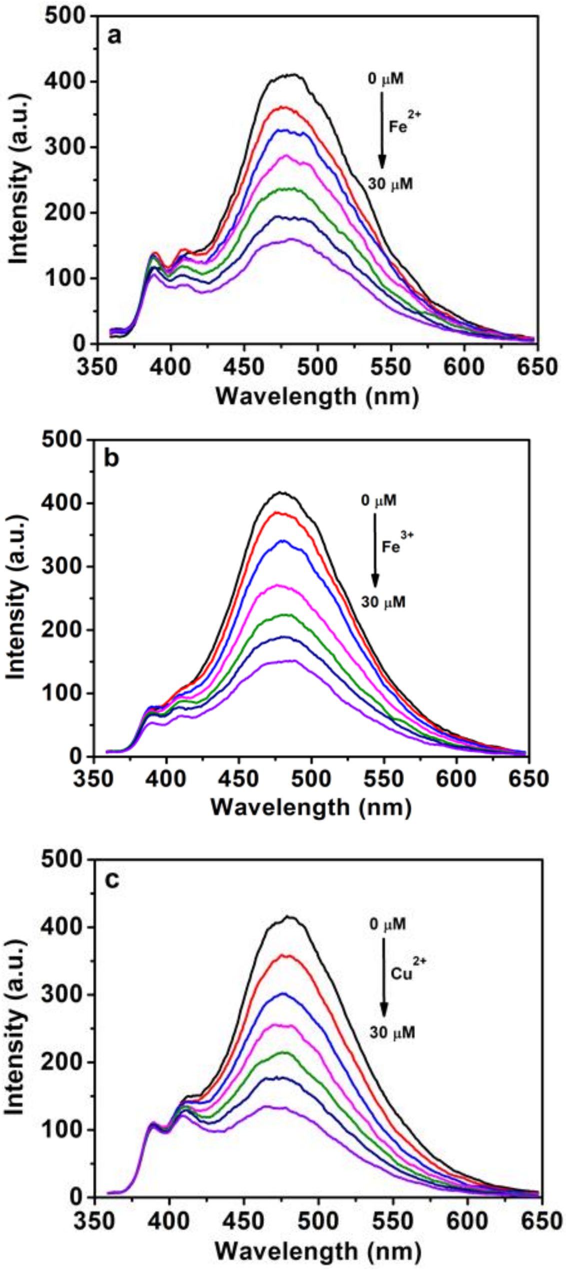

Figure 7. Fluorescence titration of **Chit-Pyr** (0.4 mg/mL) (a) Fe^{2+}, (b) Fe^{3+}, and (c) Cu^{2+} with a gradually increased concentration in DMF ($\lambda_{ex} = 345$ nm)

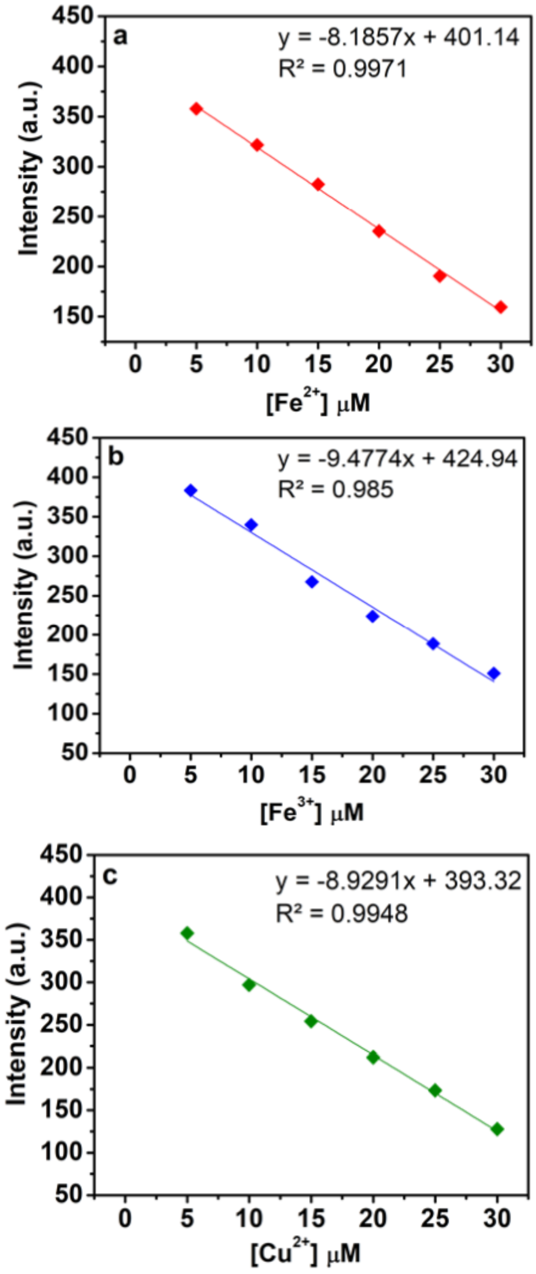

Figure 8. The linear relationship between fluorescence responses of **Chit-Pyr** and metal ions (a) Fe^{2+}, b) Fe^{3+}, and (c) Cu^{2+}.

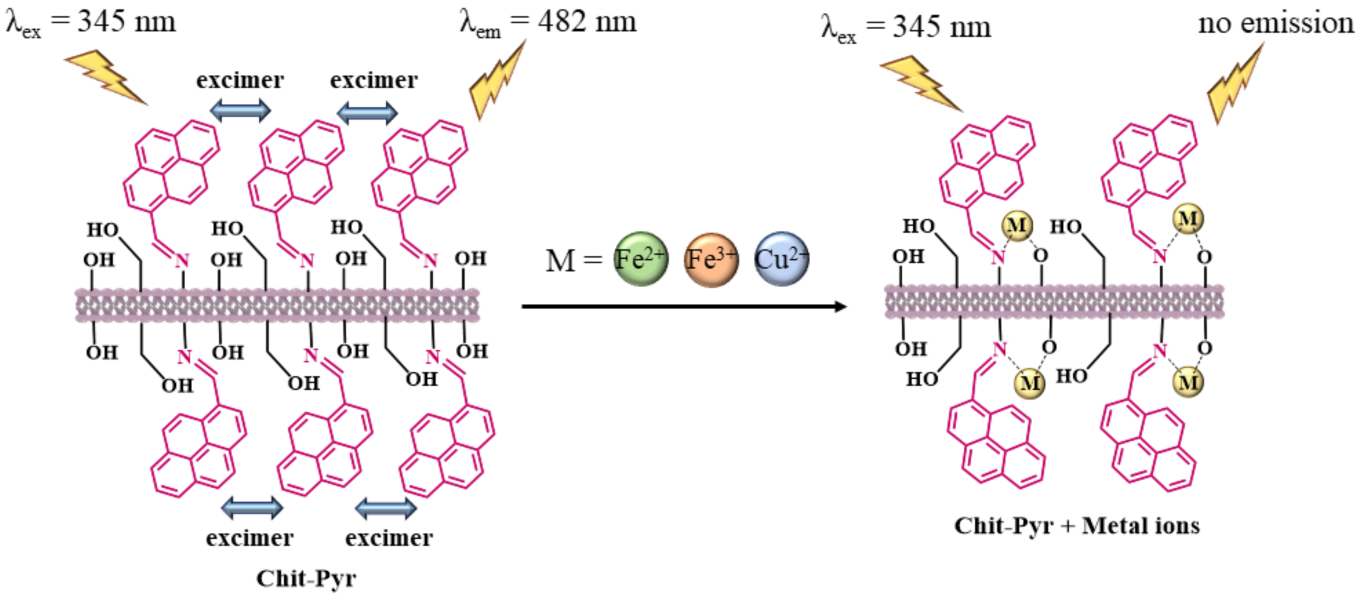

Scheme 2. Proposed “turn-off” fluorescence sensing mechanism of Fe^{2+}, Fe^{3+}, and Cu^{2+} with **Chit-Pyr**.

Heavy metals such as iron and copper, which chelate with the -OH and $-NH_2$ groups in chitosan, cause a change in the emission signal due to the photoinduced electron transfer (PET) mechanism. Electron transfer occurs from the excited compound to the electron-deficient metal ions with Lewis acid character and quenches the emission signal of the fluorescence compound [51]. The -OH groups that provide charge transfer from the ligand to the metal ion were deprotonated after the interaction of **Chit-Pyr** with Fe^{2+}, Fe^{3+}, and Cu^{2+}. The coordination between Fe^{2+}, Fe^{3+}, Cu^{2+}, and **Chit-Pyr** was accomplished through the hydroxyl oxygen atom and the imine nitrogen atom [2,52]. Scheme 2 indicates the proposed “turn-off” fluorescence sensing mechanism of Fe^{2+}, Fe^{3+}, and Cu^{2+}.

4. Conclusion

Interest in biopolymer-based fluorescent sensors is increasing, as they exhibit cost-effective, biodegradable, and environmentally friendly properties. Also, biopolymers with new properties are obtained by functionalization with alternative groups. In this study, novel, sensitive, and simple “turn-off” fluorescence studies were performed using pyrene-modified chitosan hybrid (**Chit-Pyr**) against Fe^{2+}, Fe^{3+}, and Cu^{2+} ions. FTIR, UV-Vis, TGA, and SEM were used to examine for structural, thermal, and morphological properties of **Chit-Pyr**. Photophysical properties of **Chit-Pyr** were determined by UV-Vis absorption and fluorescence studies. The selective “turn-off” fluorescence response for **Chit-Pyr** was obtained towards Fe^{2+}, Fe^{3+}, and Cu^{2+} ions in different competitive species. It is thought that this study will contribute to the preparation of stable, economical, and sustainable new hybrid biopolymers for use in fluorescence sensor studies.

Acknowledgment

The authors thank to Assoc. Prof. Dr. Ahmet Şenocak and Assoc. Prof. Dr. Süreyya Oğuz Tümay for their valuable contributions.

References

[1] P. Kumar, V. Kumar, R. Gupta, Arene-based fluorescent probes for the selective detection of iron, RSC Adv, 5, 2015, 97874–97882.

[2] X. Zhu, Y. Duan, P. Li, H. Fan, T. Han, X. Huang, A highly selective and instantaneously responsive Schiff base fluorescent sensor for the “turn-off” detection of iron(iii), iron(ii), and copper(ii) ions, Anal Methods, 11, 2019, 642–647.

[3] G.J. Park, G. R. You, Y. W. Choi, C. Kim, A naked-eye chemosensor for simultaneous detection of iron and copper ions and its copper complex for colorimetric/fluorescent sensing of cyanide, Sensor Actuat B-Chem, 229, 2016, 257–271.

[4] G. T. Selvan, C. Varadaraju, R. T. Selvan, I. V. M. V. Enoch, P. M. Selvakumar, On/Off Fluorescent Chemosensor for Selective Detection of Divalent Iron and Copper Ions: Molecular Logic Operation and Protein Binding, ACS Omega, 3, 2018, 7985–7992.

[5] A. Parsaei-Khomami, A. Badiei, Z. S. Ghavami, J. B. Ghasemi, A new fluorescence probe for simultaneous determination of Fe^{2+} and Fe^{3+} by orthogonal signal correction-principal component regression, J Mol Struct, 1252, 2022, 131978.

[6] A. Paterek, U. Mackiewicz, M. Mączewski, Iron and the heart: A paradigm shift from systemic to cardiomyocyte abnormalities, J Cell Physiol 234, 2019, 21613–21629.

[7] J. Kaplan, D. M. Ward, R. J. Crisp, C. C. Philpott, Iron-dependent metabolic remodeling in S. cerevisiae, Biochim Biophys Acta-Mol. Cell Res, 1763, 2006, 646–651.

[8] K. Pantopoulos, S. K. Porwal, A. Tartakoff, L. Devireddy, Mechanisms of Mammalian Iron Homeostasis, Biochem, 51, 2012, 5705–5724.

[9] A. M. Şenol, Y. Onganer, K. Meral, An unusual “off-on” fluorescence sensor for iron(III) detection based on fluorescein–reduced graphene oxide functionalized with polyethyleneimine, Sens Actuat B-Chem, 239, 2017, 343–351.

[10] S. O. Tümay, S.Y. Sarıkaya, S. Yeşilot, Novel iron(III) selective fluorescent probe based on synergistic effect of pyrene-triazole units on a cyclotriphosphazene scaffold and its utility in real samples, J Lumin, 196, 2018, 126–135.

[11] S. O. Tümay, M. H. Irani-nezhad, A. Khataee, Design of novel anthracene-based fluorescence sensor for sensitive and selective determination of iron in real samples, J Photoc Photobio A, 402, 2020, 112819.

[12] S. O. Tümay, E. Okutan, I. F. Sengul, E. Özcan, H. Kandemir, T. Doruk, M. Çetin, B. Çoşut, Naked-eye fluorescent sensor for Cu(II) based on indole conjugate BODIPY dye, Polyhedron, 117, 2016, 161–171.

[13] Z. Khoshbin, M. R. Housaindokht, A. Verdian, M. R. Bozorgmehr, Simultaneous detection and determination of mercury (II) and lead (II) ions through the achievement of novel functional nucleic acid-based biosensors, Biosens Bioelectron, 116, 2018, 130–147.

[14] S. García-Marco, A. Torreblanca, J.J. Lucena, Chromatographic Determination of Fe Chelated by Ethylenediamine-N-(o-hydroxyphenylacetic)-N′-(p-hydroxyphenylacetic) Acid in Commercial EDDHA/Fe^{3+} Fertilizers, J Agr Food Chem, 5, 2006, 1380–1386.

[15] N. Scheers, T. Andlid, M. Alminger, A. S. Sandberg, Determination of Fe^{2+} and Fe^{3+} in Aqueous Solutions Containing Food Chelators by Differential Pulse Anodic Stripping Voltammetry, Electroanal, 22, 2010, 1090–1096.

[16] R. Ferreira, J. Chaar, M. Baldan, N. Braga, Simultaneous voltammetric detection of Fe^{3+}, Cu^{2+}, Zn^{2+}, Pb^{2+} e Cd^{2+} in fuel ethanol using anodic stripping voltammetry and boron-doped diamond electrodes, Fuel, 291, 2021, 120104.

[17] Y. Guo, N. Huang, B. Yang, C. Wang, H. Zhuang, Q. Tian, Z. Zhai, L. Liu, X. Jiang, Hybrid diamond/graphite films as electrodes for anodic stripping voltammetry of trace Ag^{+} and Cu^{2+}, Sens Actuat B-Chem, 231, 2016, 194–202.

[18] E. Bakkaus, R. N. Collins, J.-L. Morel, B. Gouget, Anion exchange liquid chromatography–inductively coupled plasma-mass spectrometry detection of the Co^{2+}, Cu^{2+}, Fe^{3+} and Ni^{2+} complexes of mugineic and deoxymugineic acid, J Chromatogr A, 1129, 2006, 208–215.

[19] A. Spolaor, P. Vallelonga, J. Gabrieli, G. Cozzi, C. Boutron, C. Barbante, Determination of Fe^{2+} and Fe^{3+} species by FIA-CRC-ICP-MS in Antarctic ice samples, J Anal Atom Spectrom, 27, 2012, 310–317.

[20] M. Yaman, G. Kaya, Speciation of iron (II) and (III) by using solvent extraction and flame atomic absorption spectrometry, Anal Chim Acta, 540, 2005, 77–81.

[21] M. Ghaedi, K. Niknam, K. Taheri, H. Hossainian, M. Soylak, Flame atomic absorption spectrometric determination of copper, zinc and manganese after solid-phase extraction using 2,6-dichlorophenyl-3,3-bis(indolyl)methane loaded on Amberlite XAD-16, Food Chem Toxicol, 48, 2010, 891–897.

[22] T. Verma, P. Verma, U. P. Singh, A multi responsive phosphonic acid based fluorescent sensor for sensing Fe^{3+}, benzaldehyde and antibiotics, Microchem J, 191, 2023, 108771.

[23] S. H. Park, N. Kwon, J. H. Lee, J. Yoon, I. Shin, Synthetic ratiometric fluorescent probes for detection of ions, Chem Soc Rev, 49, 2020, 143–179.

[24] W. Wang, L. Chai, X. Chen, Z. Li, L. Feng, W. Hu, H. Li, G. Yang, Imaging changes in the polarity of lipid droplets during NAFLD-Induced ferroptosis via a red-emitting fluorescent probe with a large Stokes shift, Biosens Bioelectron, 231, 2023, 115289.

[25] P. R. Yaashikaa, P. S. Kumar, S. Karishma, Review on biopolymers and composites – Evolving material as adsorbents in removal of environmental pollutants, Environ Res, 212, 2022, 113114.

[26] A. Das, T. Ringu, S. Ghosh, N. Pramanik, A comprehensive review on recent advances in preparation, physicochemical characterization, and bioengineering applications of biopolymers, Polym Bull, 2022, 1–66.

[27] M. Nasrollahzadeh, M. Sajjadi, S. Iravani, R. S. Varma, Starch, cellulose, pectin, gum, alginate, chitin and chitosan derived (nano)materials for sustainable water treatment: A review, Carbohyd Polym, 251, 2021, 116986.

[28] W. Wang, C. Xue, X. Mao, Chitosan: Structural modification, biological activity and application, Int J Biol Macromol, 164, 2020, 4532–4546.

[29] R. Priyadarshi, J.W. Rhim, Chitosan-based biodegradable functional films for food packaging applications, Innov Food Sci Emerg, 62, 2020, 102346.

[30] Y. Chen, Y. Liu, Q. Dong, C. Xu, S. Deng, Y. Kang, M. Fan, L. Li, Application of functionalized chitosan in food: A review, Int J Biol Macromol, 235, 2023, 123716.

[31] P. S. B, D. Selvakumar, K. Kadirvelu, N. S. Kumar, Chitosan as an environment friendly biomaterial – a review on recent modifications and applications, Int J Biol Macromol, 150, 2020, 1072–1083.

[32] M. Zhang, F. Zhang, C. Li , H. An, T. Wan, P. Zhang, Application of Chitosan and Its Derivative Polymers in Clinical Medicine and Agriculture, Polymers-Basel, 14, 2022, 958.

[33] R. Jayakumar, M. Prabaharan, S.V. Nair, S. Tokura, H. Tamura, N. Selvamurugan, Novel carboxymethyl derivatives of chitin and chitosan materials and their biomedical applications, Prog Mater Sci, 55, 2010, 675–709.

[34] B. I. Andreica, X. Cheng, L. Marin, Quaternary ammonium salts of chitosan. A critical overview on the synthesis and properties generated by quaternization, Eur Polym J, 139, 2020, 110016.

[35] H. A.Alidağı, S. O. Tümay, A. Şenocak, S. Yeşilot, Pyrene functionalized cyclotriphosphazene-based dyes: Synthesis, intramolecular excimer formation, and fluorescence receptor for the detection of nitro-aromatic compounds, Dyes Pigments, 153, 2018, 172–181.

[36] V. Kumar, B. Sk, S. Kundu, A.Patra, Dynamic and static excimer: a versatile platform for single component white-light emission and chelation-enhanced fluorescence, J Mater Chem C, 6, 2018, 12086–12094.

[37] L. Gai, H. Chen, B. Zou, H. Lu, G. Lai, Z. Li, Z. Shen, Ratiometric fluorescence chemodosimeters for fluoride anion based on pyrene excimer/monomer transformation, Chem Commun, 48, 2012, 10721–10723.

[38] M. Belovari, D. Nestić, I. Marić, D. Majhen, M. Cametti, Z. Džolić, Photophysical characterization and the self-assembly properties of mono- and bis-pyrene derivatives for cell imaging applications, New J Chem, 46, 2022, 22518–22524.

[39] S. Jatunov, A. Franconetti, R. Prado-Gotor, A. Heras, M. Mengíbar, F. Cabrera-Escribano, Fluorescent imino and secondary amino chitosans as potential sensing biomaterials, Carbohyd Polym, 123, 2015, 288–296.

[40] A. Franconetti, P. Domínguez-Rodríguez, D. Lara-García, R. Prado-Gotor, F. Cabrera-Escribano, Native and modified chitosan-based hydrogels as green heterogeneous organocatalysts for imine-mediated Knoevenagel condensation, Appl Catal A-Gen, 517, 2016, 176–186.

[41] P. Sirajunnisa, C. Sabna, A. Aswin, S. Prathapan, G. S. Sailaja, Lawsone-bentonite hybrid systems for pH-dependent sustained release of ciprofloxacin, New J Chem, 46, 2022, 9560–9571.

[42] H. M. Lee, M. H. Kim, Y. I. Yoon, W. H. Park, Fluorescent Property of Chitosan Oligomer and Its Application as a Metal Ion Sensor, Mar Drugs, 15, 2017, 105.

[43] D. Wang, L. Marin, X. Cheng, Fluorescent chitosan-BODIPY macromolecular chemosensors for detection and removal of Hg^{2+} and Fe^{3+} ions, Int J Biol Macromol, 198, 2022, 194–203.

[44] Z. Meng, Z. Wang, Y. Liang, G. Zhou, X. Li, X. Xu, Y. Yang, S. Wang, A naphthalimide functionalized chitosan-based fluorescent probe for specific detection and efficient adsorption, Int J Biol Macromol, 239, 2023, 124261.

[45] S. O. Tümay, V. Şanko, E. Demirbaş, A. Şenocak, Fluorescence determination of trace level of cadmium with pyrene modified nanocrystalline cellulose in food and soil samples, Food Chem Toxicol, 146, 2020, 11184.

[46] M. A. Ahghari, M. R. Ahghari, M. Kamalzare, A. Maleki, Design, synthesis, and characterization of novel eco-friendly chitosan-

$AgIO_3$ bionanocomposite and study its antibacterial activity, Sci Rep-UK, 12, 2022, 10491.

[47] T. Jiang, C. Wang, W. Liu, Y. Li, Y. Luan, P. Liu, Optimization and characterization of lemon essential oil entrapped from chitosan/cellulose nanocrystals microcapsules, J Appl Polym Sci, 138, 2021, 51265.

[48] S. O. Tümay, V. Şanko, A. Şenocak, E. Demirbaş, A hybrid nanosensor based on novel fluorescent iron oxide nanoparticles for highly selective determination of Hg^{2+} ions in environmental samples, New J Chem, 45, 2021, 14495–14507.

[49] H. Ardic Alidagi, S. O. Tümay, A. Şenocak, Ö. F. Çiftbudak, B. Çoşut, S. Yeşilot, Constitutional isomers of dendrimer-like pyrene substituted cyclotriphosphazenes: synthesis, theoretical calculations, and use as fluorescence receptors for the detection of explosive nitroaromatics, New J Chem, 43, 2019, 16738–16747.

[50] P. K. Lekha, E. Prasad, Tunable Emission of Static Excimer in a Pyrene-Modified Polyamidoamine Dendrimer Aggregate through Positive Solvatochromism, Eur J Chem, 17, 2011, 8609–8617.

[51] H. Gupta, K. Kaur, R. Singh, V. Kaur, Chitosan Schiff base for the spectrofluorimetric analysis of E-waste toxins: Pentabromophenol, Fe^{3+}, and Cu^{2+} ions, Cellulose, 30, 2023, 1381–1397.

[52] T. Sun, Q. Niu, T. Li, Z. Guo, H. Liu, A simple, reversible, colorimetric and water-soluble fluorescent chemosensor for the naked-eye detection of Cu^{2+} in ~100% aqueous media and application to real samples, Spectrochim Acta A, 188, 2018, 411–417.